Sensors and Actuators A 188 (2012) 203–211

Contents lists available at SciVerse ScienceDirect

Sensors and Actuators A: Physical

journal homepage: www.elsevier.com/locate/sna

A role of silica nanoparticles in layer-by-layer self-assembled carbon nanotube and In_2O_3 nanoparticle thin-film pH sensors: Tunable sensitivity and linearity

Dongjin Lee [1], Tianhong Cui *

Department of Mechanical Engineering, University of Minnesota at Twin Cities, 111 Church St. S.E., Minneapolis, MN 55455, USA

ARTICLE INFO

Article history:
Received 29 September 2011
Received in revised form 2 January 2012
Accepted 4 January 2012
Available online 12 January 2012

Keywords:
Carbon nanotube (CNT)
Indium oxide (In_2O_3) nanoparticle
Silica (SiO_2) nanoparticle
Chemoresistor
ISFET
pH sensor

ABSTRACT

A role of the dielectric silica nanoparticle (SiO_2 NP) in nanomaterial chemoresistors and ion-sensitive field-effect transistors (ISFET) is demonstrated in this study. Single-walled carbon nanotubes (SWCNT) and indium oxide nanoparticles (In_2O_3 NP) are layer-by-layer self-assembled alternately with oppositely charged polyelectrolytes, respectively. Nanomaterial multilayer thin-film is patterned using photolithography and electrochemically characterized in various pH buffers. The pH sensors are implemented as resistor and transistor in absence and presence of SiO_2 NP layer. We observed tunable sensitivity and linearity of output current flowing through the conducting channel in SWCNT chemoresistor and ISFET. The role of SiO_2 NP is proven to modulate and linearize the sensitivity to pH. The linearization is attributed to a positive shift in pH gating voltage in p-type semiconducting SWCNTs. On the other hand, a tunable sensitivity is observed whereas the linearization is not demonstrated in In_2O_3 NP ISFETs. The increased sensitivity with SiO_2 NP in acidic region is caused by a positive shift in gate voltage due to the protonation of the surface hydroxyl groups. This facile modulation and linearization of the electrochemical sensitivity in semiconducting nanomaterial thin-film device by means of the additional SiO_2 NP layer is useful for developing various functional nanomaterial-based biosensors.

1. Introduction

The nanomaterial is a good candidate for developing solid-state pH electrode due to the unique electrochemical property. A series of nanomaterial-based ion-sensitive field-effect transistors (ISFET) was reported as pH [1,2] and acetylcholine sensors [3,4] possessing silica nanoparticles (SiO_2 NP) as a dielectric layer on top of semiconducting nanomaterial thin-film. The authors argued that SiO_2 NPs acted as a gate dielectric layer in the conventional FET structure. However, the self-assembled SiO_2 NP thin-film is porous, so that it could not prevent the analyte solution penetrating into the semiconducting layer perfectly as in conventional ISFETs. In consequence, it is questionable whether the chemical information such as pH or analyte concentration is transformed only through semiconducting layer or together with SiO_2 NP layer. In addition, single-walled carbon nanotube (SWCNT) thin-film without any dielectric layer showed the pH-sensitive electrochemical properties [5], since the proximal ionic composition change [5–7] and protonation/deprotonation of the surface functional groups of semiconducting nanomaterials [8,9] influence the electrical properties of nanomaterial thin-film itself. This suggested the elimination of gate dielectric layer. Therefore, the reason for the existence of SiO_2 NP layer in all-nanomaterial ISFETs has not been elucidated so far.

In case of the conventional ISFET with a dielectric, pH decrease in sample solution induces more positive charges on the dielectric due to the protonation of surface hydroxyl group. This plays the role of positive shift in the gate voltage, resulting in decreasing conductance in p-type semiconducting material in a sense of conventional FET. However, SWCNT ISFET with porous SiO_2 NP layer actually showed the opposite behavior, which was linearly increasing conductance with decreasing pH [2]. It meant the protonation/deprotonation of carboxylic groups on SWCNTs played a dominant role to determine the overall behavior that was decreasing conductance with pH [8]. On contrary, the penetration of the sample solution might be beneficial to n-type semiconducting materials, e.g. indium oxide (In_2O_3) nanoparticles [1], since the gate voltage shift by SiO_2 NP layer is positive. Nonetheless, this dual effect of solution pH on the conductance of semiconducting nanomaterials in the presence of SiO_2 NPs makes it difficult to estimate the electrochemical behavior of nanomaterial devices, exploit excellent properties, and design novel nanostructures that might have a higher performance.

Although much effort has been made on demonstrating biosensing applications of nanomaterials, no systematic study has been

* Corresponding author. Tel.: +1 612 626 1636; fax: +1 612 625 6069.
E-mail address: tcui@me.umn.edu (T. Cui).
[1] Current address: Department of Mechanical Engineering, Korea Advanced Institute of Science and Technology 291 Daehak-ro, Yuseong-gu, Daejeon 305-701, Korea.

0924-4247/$ – see front matter © 2012 Elsevier B.V. All rights reserved.
doi:10.1016/j.sna.2012.01.004

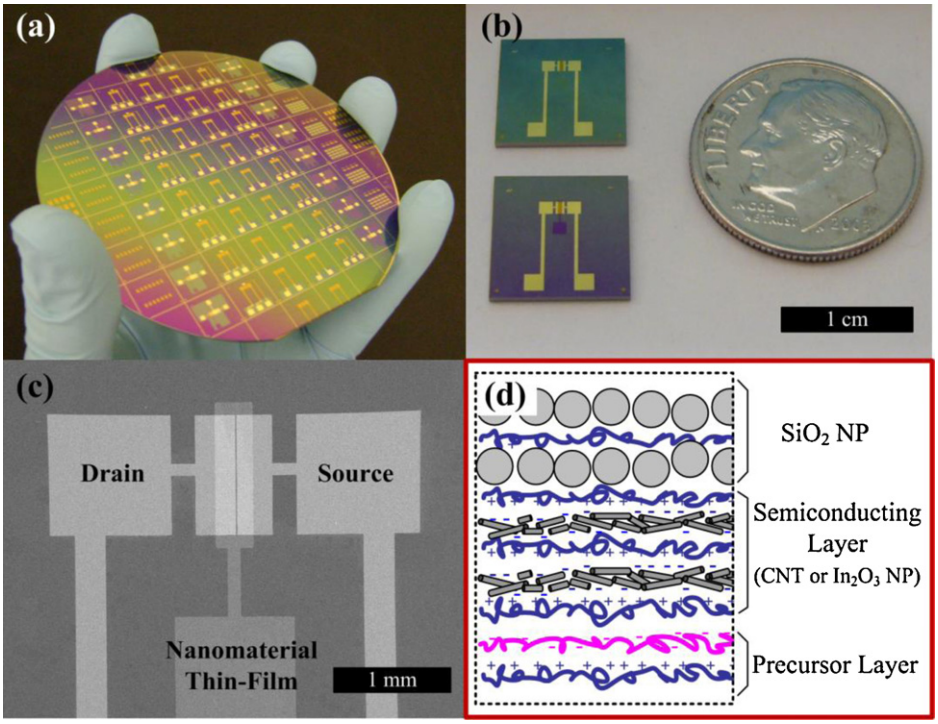

Fig. 1. Layer-by-layer self-assembled nanomaterial thin-film pH sensors: (a) 4 in. wafer scale fabrication, (b) diced individual sensing chips in size of 1 cm by 1 cm, (c) SEM image of the electrode patterns and nanomaterial thin-film, and (d) hierarchical structure of nanomaterial thin-film composed of precursor layer of $(PDDA/PSS)_2$, semiconducting layer of SWCNT or In_2O_3 NP film, and silica nanoparticle layer.

reported yet regarding the electrochemical pH transducing properties of nanomaterial thin-film. We demonstrate in this report that pH sensitivity of the nanomaterial thin-film chemoresistor and ISFETs is tunable simply by depositing SiO_2 NP layer on top of semiconducting nanomaterial multilayer fabricated by layer-by-layer (LbL) self-assembly. We used the thin-film of SWCNTs and In_2O_3 NPs as a semiconducting nanomaterial. A new analysis on the pH-dependent conductance of SWCNT and In_2O_3 NP chemoresistors and ISFETs was performed, and the role of SiO_2 NPs layer was elucidated. Finally, we showed that the role of SiO_2 NPs in both SWCNT chemoresistors and ISFETs is to tune and linearize the pH sensitivity without complex wet chemistry. Although the linearization was not observed in In_2O_3 ISFETs, the tunable sensitivity with SiO_2 NPs particularly in acidic region was clearly demonstrated. The SiO_2 NP layer on top of the semiconducting layer plays the role of the charge collector, influencing the conductance of the semiconducting layer. In conjunction with a facile integration of SiO_2 NP, the tunable electrochemical properties of nanomaterial thin-film could be used for developing a variety of electrochemical biosensors.

2. Experiments

2.1. Materials

SWCNT (purity: 90% of SWCNT and 95% of CNT, diameter: 1–2 nm, length: 5–30 μm, SSA: 300–380 m^2/g) was purchased from Nanostructured & Amorphous Materials, Inc. and chemically functionalized in concentrated acids as done previously [6,10]. The resulting aqueous SWCNT dispersion had the final concentration of 0.6 mg/ml and pH of 5.5. In_2O_3 particle (In_2O_3 NP), aqueous polydiallyldimethylammonium chloride (PDDA, M_w = 200–350k) and sodium polystylenesulfonate (PSS, M_w = 70k) were obtained from Sigma–Aldrich. In_2O_3 NPs were dispersed into 12 mM HCl (pH 3.9) aqueous solution with a concentration of 50 mg/ml. PDDA and PSS were diluted to have a concentration of 1.4 and 0.3 wt%, respectively, with 0.5 M sodium chloride (NaCl). Another set of PSS solution (PSS2) was prepared by adjusting the pH of PSS solution to 3.9 using HCl to preserve the surface charge of In_2O_3 NPs in the PSS2 solution. As-received colloidal silica nanoparticles (SNOWTEX®-XL, Nissan Chemical America Corp.) of 4 g was diluted to 100 mL of deionized water (DIH_2O) resulting in a concentration of 16 mg/ml with pH 7.0. The pH buffers were formulated using $NaH_2PO_4{\cdot}H_2O$ and $Na_2HPO_4{\cdot}7H_2O$ so that the resulting pH ranged from 5 to 9, which was targeted for biosensing application.

3. Device fabrication

Nanomaterial thin-film devices were fabricated following the procedure previously reported [5,8]. Chromium (Cr, 300 Å) and gold (Au, 1000 Å) were electron-beam evaporated on a 4 in. silicon wafer with thermally grown oxide 2 μm thick. Photolithography was used to fabricate source and drain electrodes. The conducting channel dimension was 1 mm wide and 10 μm long. Another lithographic patterning was performed for lift-off mask layer of photoresist in order to confine nanomaterial thin-film on the conducting channel. O_2 plasma at a power of 100 W and O_2 flow rate of 100 sccm was applied for 1 min to change the surface hydrophilic for the subsequent assembly of nanomaterials. Then, LbL assembly of nanomaterials was conducted on the wafer scale under atmospheric pressure and room temperature. SWCNT was assembled alternately with positively charged PDDA following a sequence of [PDDA (10 min) + PSS (10 min)]$_2$ + [PDDA (10 min) + SWCNT (15 min)]$_5$. On the other hand, In_2O_3 NPs were assembled alternately with PSS2 with a sequence of [PDDA (10 min) + PSS (10 min)]$_2$ + [In_2O_3 NP (14 min) + PSS2 (10 min)]$_5$. Two kinds of nanomaterial thin-film were covered with the additional dielectric layer of [PDDA (10 min) + SiO_2 NP (4 min)]$_6$ to compare the electrochemical sensitivity to pH buffers in the absence and presence of silica nanoparticles. Two bilayers of (PDDA/PSS) were to enhance the surface charge for functional

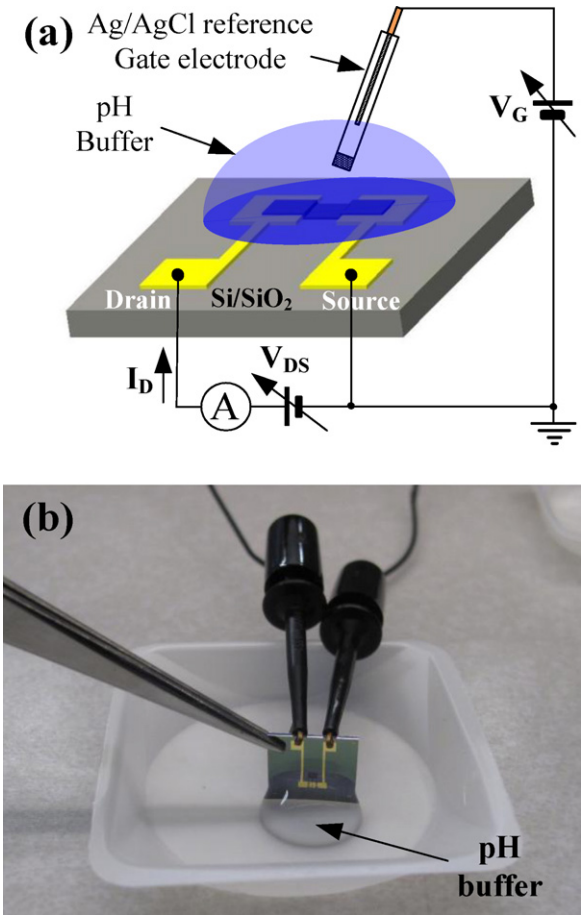

Fig. 2. Electrochemical pH sensing scheme:(a) schematic of device characterization as chemoresistor and ISFET in absence and presence of external Ag/AgCl reference electrode and (b) exemplary photograph of chemoresistor characterization: two terminals are connected to semiconductor parameter analyzer.

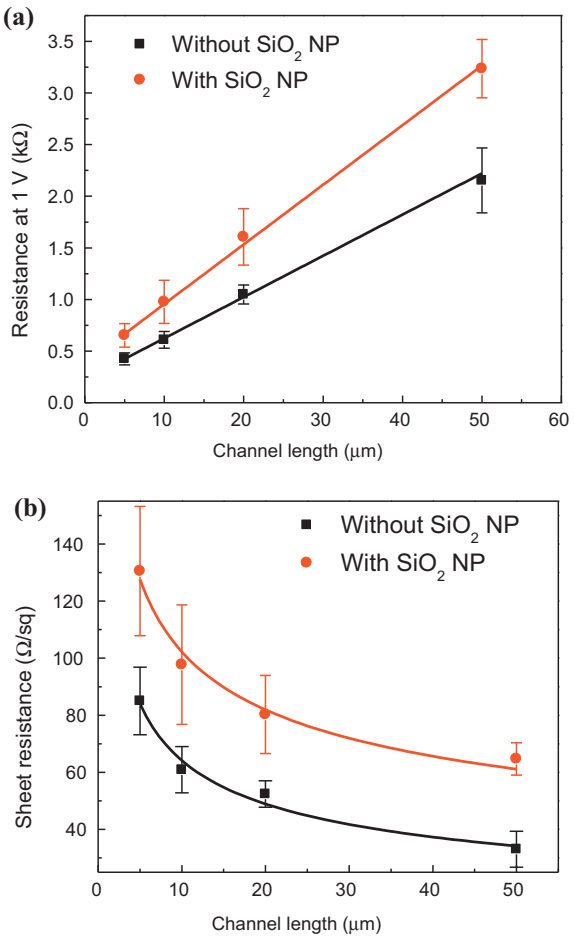

Fig. 4. Resistances (a) and sheet resistances (b) of SWCNT resistors with and without SiO_2 NP on variable channel lengths of 5, 10, 20, and 50 μm with the fixed width of 1 mm. Error bars indicate the standard deviation.

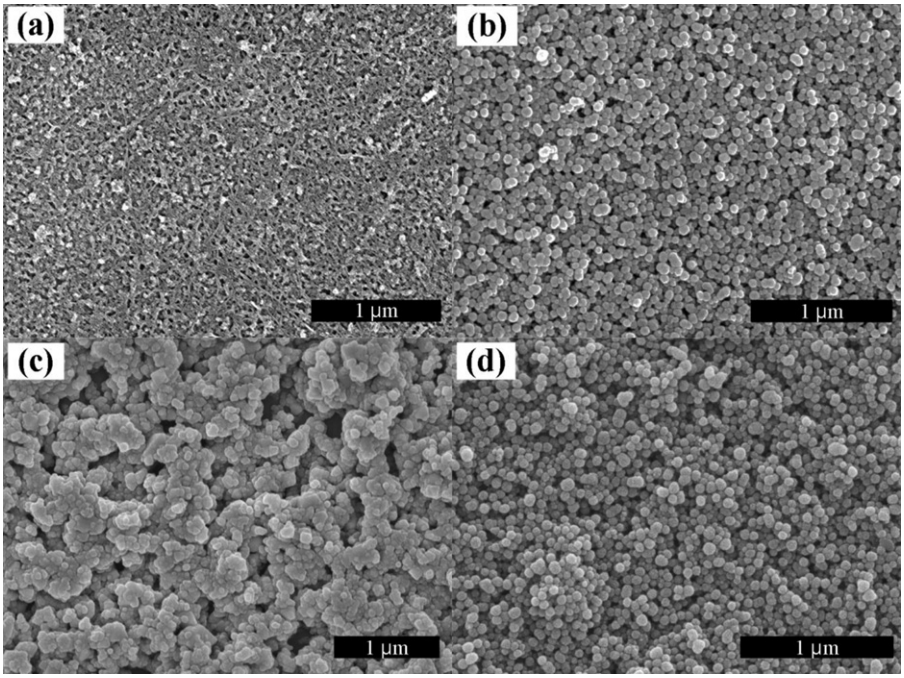

Fig. 3. SEM images of SWCNT (a) and SiO_2 NP (b) surfaces in SWCNT ISFETs, and In_2O_3 NP (c) and SiO_2 NP (d) surfaces in In_2O_3 NP ISFETs: the differences between (b) and (d) is surface roughness induced by underlying SWCNT and In_2O_3 NP multilayer.

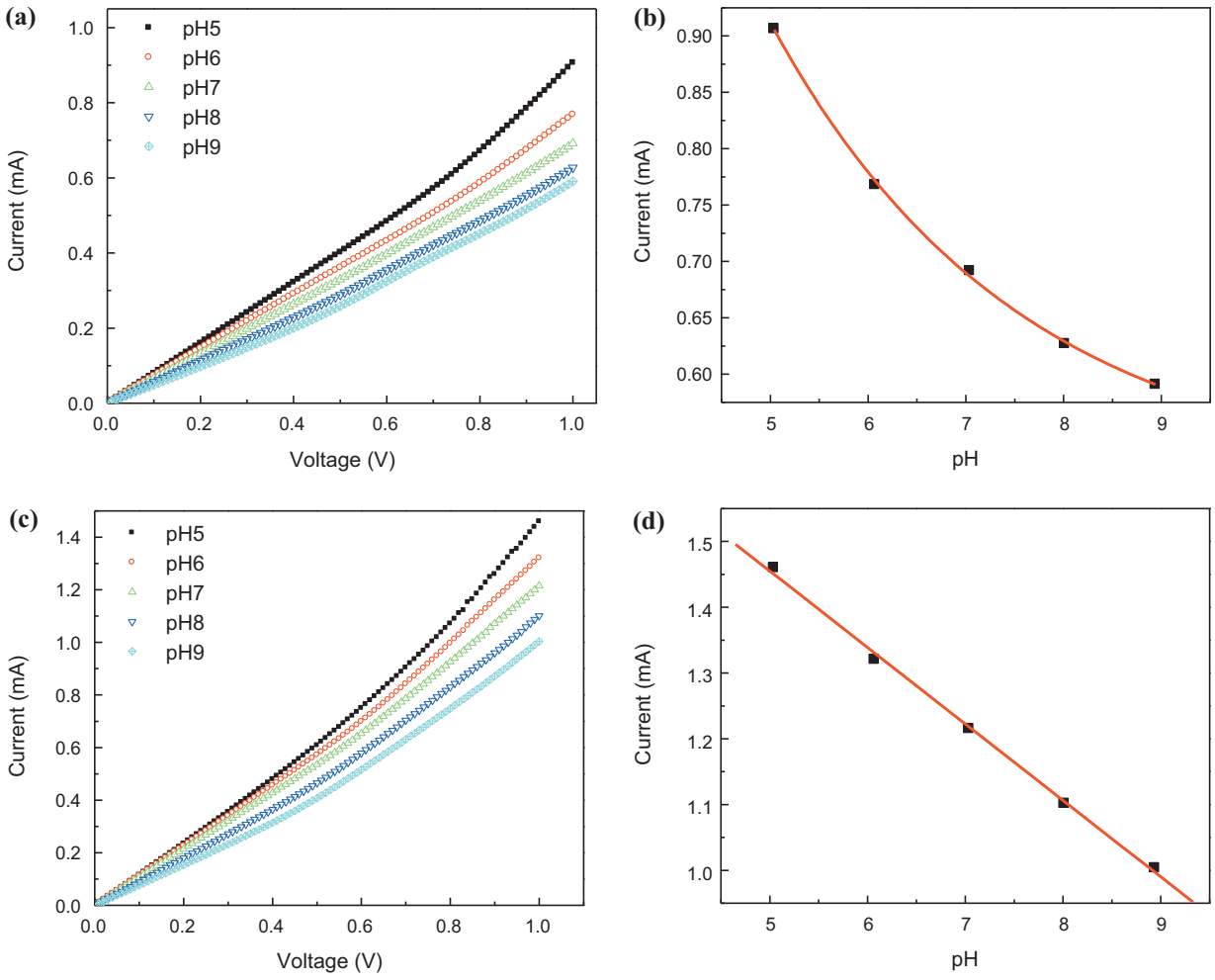

Fig. 5. A typical pH sensitivity of SWCNT chemoresistor in the absence (a and b) and presence (c and d) of SiO_2 NP: (a and c) *I–V* curves at different pH buffers, (b and d) pH-responsive currents at the bias voltage of 1 V.

nanomaterial thin-film. Finally, lift-off mask layer of photoresist was dissolved in acetone with an aid of ultrasonication to leave thin-film only on the conducting channel, followed by dicing into individual chips.

4. pH testing

The SWCNT multilayer device was considered either resistor or ISFET, while the In_2O_3 NP multilayer device was considered ISFET only when they were characterized electrically in pH buffers. The miniaturized Ag/AgCl reference electrode (Cypress Systems, EE008) with an internal filling solution of 3 M KCl was used as a gate to provide the sample solution with the stable electrical potential. After the terminals were connected to the semiconductor parameter analyzer (HP4145B), the electrical characterization was performed. During the characterization, the Ag/AgCl reference gate electrode and the readout wires from source and drain electrode were fixed to the external frame to prevent the relative motion. At this time the distance between sensor surface and the tip of reference electrode was about 5 mm. A pipette was used to add 300 μl of pH buffers on the sensor surface with reference electrode immersed. The sensors were incubated in each pH buffer solution for 1 min.

In chemoresistor scheme in absence of Ag/AgCl reference electrode, *I–V* measurement was performed at pH buffers on the bias voltage of 0–1 V and the currents at the fixed bias voltage were depicted as a function of pH. In ISFET scheme, on the other hand, the external Ag/AgCl reference electrode was used to apply gate voltage. The drain-to-source voltage (V_{DS}) was scanned from 0 to 1 V at the variable gate voltage (V_G), the drain currents (I_D) were obtained at pH buffers. The extracted I_D was illustrated versus pH at the fixed V_G and V_{DS}. A dozen of devices were characterized, and I_D obtained was normalized and averaged.

5. Results and discussion

The fabricated nanomaterial thin-film pH sensors are depicted in Fig. 1. The combination of photolithography and layer-by-layer assembly enables scale-up fabrication of devices over the 4 in. wafer level as shown in Fig. 1(a). The diced single device with two terminals is in size of 1 cm by 1 cm as shown in Fig. 1(b). The fabricated drain and source electrode patterns are shown in Fig. 1(c). The nanomaterial (SWCNT or In_2O_3 NP) thin-film is confined on the conducting channel as observed in Fig. 1(b) and (c) to minimize side electrochemical reaction on the area other than the conducting channel. The thin-film hierarchy is shown in Fig. 1(d), where three distinct parts are observed: precursor of $(PDDA/PSS)_2$ for charge enhancement of the substrate, functional semiconducting layer of SWCNT or In_2O_3 NP multilayer, and dielectric silica nanoparticles.

The fabricated devices are electrochemically characterized in various pH buffers in absence and presence of Ag/AgCl reference electrode as shown in Fig. 2. Without the reference electrode, devices act as resistor while they function as transistors with the reference electrode as shown in Fig. 2(a). In chemoresistor scheme, a bias voltage is applied to the drain electrode with the source

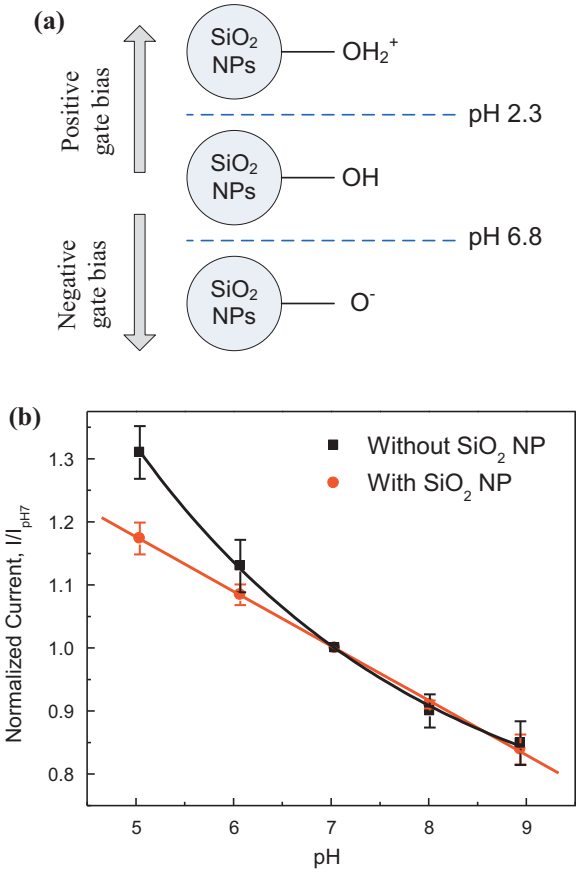

Fig. 6. General pH sensitivity behavior of SWCNT chemoresistors without and without SiO_2 NP: (a) scheme of pH-responsive surface functional groups in SiO_2 NPs and (b) pH sensitivity of SWCNT chemoresistor normalized with the current at pH 7 in the presence and absence of SiO_2 NPs. Error bars denote the standard deviation.

electrode grounded, and the current (I_D) flowing through the nanomaterial thin-film was measured. An exemplary photograph of chemoresistor characterization is shown in Fig. 2(b). At the same bias voltage, different current levels were found depending on the pH buffer primarily due to the mutation in the electrical property of nanomaterial thin-film. The conductance shift due to the sample solutions can be considered as a kind of gate voltage from the conventional semiconductor point of view, although determining *on/off* state and charge carrier mobility is not straightforward. On the other hand, chemoresistors can be characterized with an ISFET characterization scheme with the aid of the external Ag/AgCl reference electrode. The gate voltage is applied to boost the effect of the sample solutions on the conductance change of the nanomaterial multilayer. It has been demonstrated that the use of an external gate electrode increases sensitivity, but decreases the sensor resolution compared to chemoresistors [4].

The surface of self-assembled SWCNT, In_2O_3 NP and SiO_2 NP layers was characterized in field emission gun scanning electron microscope (FE-SEM, Jeol 6700). The SWCNT and In_2O_3 NP semiconducting layers are shown in Fig. 3(a) and (c), and SiO_2 NP layer on top of SWCNT and In_2O_3 NP are shown in Fig. 3(b) and (d), respectively. The different surface morphology is observed in (b) and (d) presumably due to the underlying semiconducting SWCNT and In_2O_3 NP layer. The random network of SWCNTs is observed in Fig. 3(a) and the additional layer of silica covers well over the SWCNT layer as shown in Fig. 3(b). The presence of metallic SWCNTs deteriorates the functionality of solid-state FETs, resulting in a positive threshold voltage, high leakage current between drain and source electrodes, and low *on/off* ratio [11]. However, it is valuable for chemical and biological sensors, since they can yield the output signal sensitive to the proximal ionic environment [5]. In_2O_3 NP multilayer comprises a complex percolation path where the interparticle contact resistance plays a dominant role in an equivalent circuit. The SWCNT multilayer device was considered either resistor due to the presence of metallic SWCNTs or ISFET due to the semiconducting ones, while the In_2O_3 NP multilayer device should be considered ISFET only since In_2O_3 is the semiconducting material with the bandgap of 3.2 eV [12].

First of all, *I–V* measurement was performed for SWCNT resistors with and without SiO_2 NP at the atmosphere. The devices showed a linear relationship between the current and voltage in both forward and negative biases, suggesting the ohmic contact between SWCNT film and metal electrodes, and among SWCNTs. The resistance was extracted at the bias voltage of 1 V, and results are shown in Fig. 4, where error bars are embedded as the standard deviation. The resistance on the variable channel lengths of 5, 10, 20, and 50 μm with a fixed width of 1 mm is shown in Fig. 4(a). The resistance of devices with SiO_2 NP is 50–60% higher than that of devices without SiO_2 NP. The surface adsorption onto SWCNTs seemed to be the primary reason for the increased resistance due to the reduced free surface permitting less charge carrier transfer. The resistivity is calculated from the slop of fitted lines based on the assumption that the thickness of the film is 38 nm [13]. The resistances of the thin-film are found to fit to $R = 39.94\,\Omega/\mu m \times L + 225\,\Omega$ and $R = 57.76\,\Omega/\mu m \times L + 378\,\Omega$ for devices without and with SiO_2 NP, respectively, where L is the channel length. The resistivity found is 0.15 and 0.22 Ω cm, and contact resistances between metal electrodes and SWCNT film were found as 113 and 189 Ω for the resistors in the absence and presence of SiO_2 NP. The resistivity of SWCNT thin-film with SiO_2 NP on top is 45% greater than that of the film without SiO_2 NP. The sheet resistance versus the channel length is shown in Fig. 4(b) in order to compare the sheet resistance on the different channel length. The sheet resistance of SWCNT multilayer with SiO_2 NP is also 50–60% higher than that of SWCNT without SiO_2 NP. The sheet resistance calculated from the resistivity determined in Fig. 4(a) was 39.94 and 57.76 Ω/□ without and with SiO_2 NP, respectively. It is clearly noted, furthermore, that the sheet resistance of CNT film fabricated as bulky paper in the vacuum filtering showed 356 Ω/□ [14], which is greater than the LbL assembled film in this work. The chemically functionalized SWCNTs showed lower sheet resistance of 200 Ω/□ [15], but it is still bigger than the sheet resistance found in this work. The sheet resistance of SWCNT film is known to be dependent on the amount of SWCNTs [14,16], which means a high loading of SWCNTs can be implemented using LbL self-assembly. However, the sheet resistance decreases as the channel length increases regardless of the existence of SiO_2 NPs, reaching the values calculated from resistivity.

A typical pH sensitivity of SWCNT chemoresistors without and with SiO_2 NP layer is shown in Fig. 5. *I–V* curves at different pH buffers are shown in Fig. 5(a) and (c), and the currents were extracted from the bias voltage of 1 V and replotted as a function of pH as shown in Fig. 5(b) and (d). The pH-responsive current without SiO_2 NP layer exhibits the behavior well fit to exponential function. On the other hand, pH sensitivity from the SWCNT resistor with SiO_2 NP layer shows a linear response. The exponential behavior without SiO_2 NP layer is in good agreement with the previously reported results [8,10]. It is obvious that the device with SiO_2 NP had higher resistance at the atmosphere than the one without SiO_2 NP, but higher currents at pH buffers. This conflicting phenomenon may come from 2 aspects. The significant swelling effect in SWCNT multilayer is found without SiO_2 NP layer, the effect of which might decrease with the presence of SiO_2 NP layer. Secondly, the accumulation mode of semiconducting channel might be induced due to the charges on SiO_2 NP layer. Indeed, the SiO_2 NP layer might play an

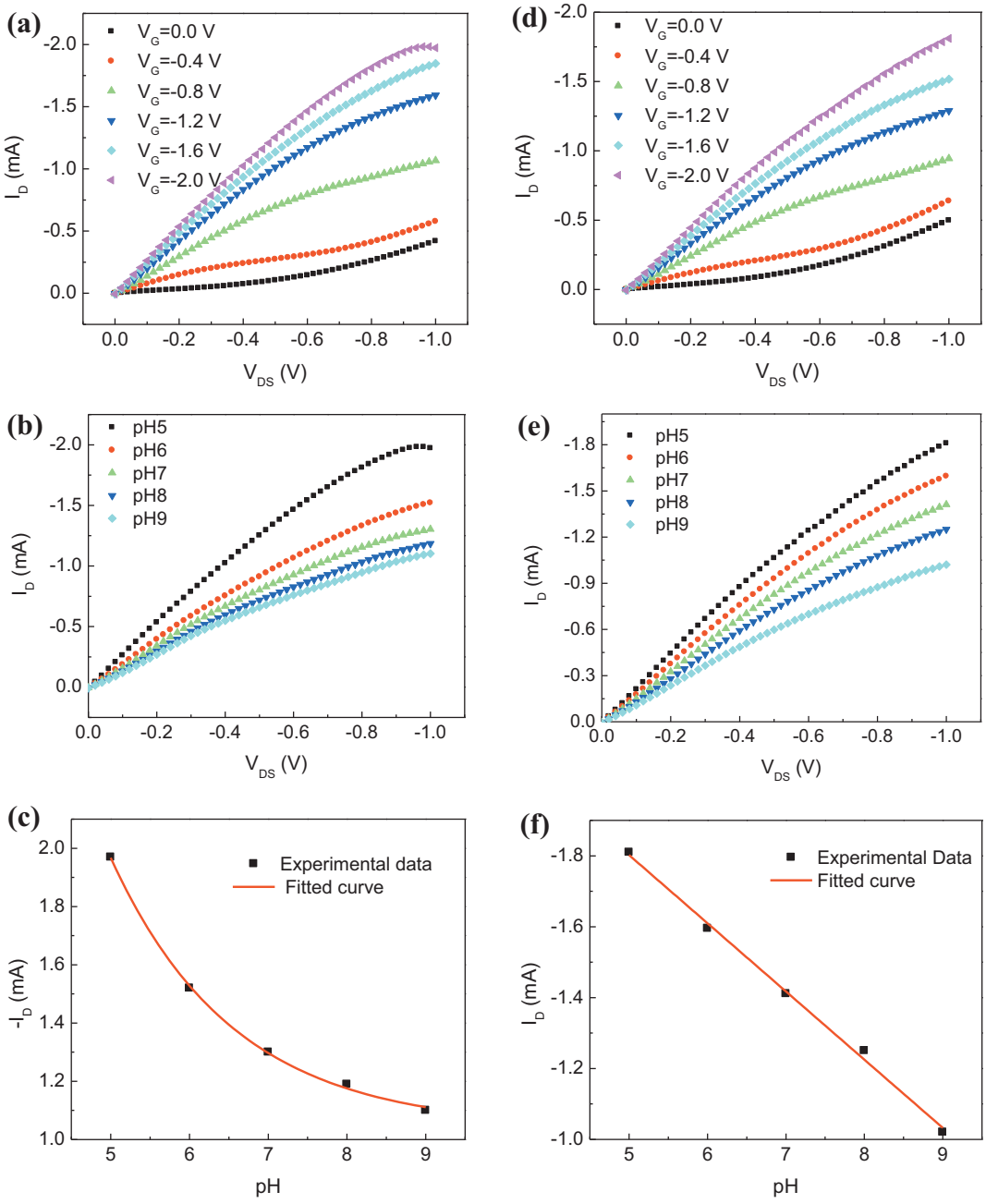

Fig. 7. A typical pH sensitivity of SWCNT ISFETs in the absence (a–c) and presence (d–f) of SiO_2 NP: (a and d) field-effect test at pH 5 buffer, (b and e) drain currents at different pH buffers at the fixed $V_G = -2.0$ V, and (c and f) pH-responsive drain current at the fixed $V_G = -2.0$ V and $V_{DS} = -1.0$ V.

important role of modulating pH sensitivity of SWCNT chemoresistors.

The multiple SWCNT chemoresistors were tested, and the currents were normalized with the current at pH 7 and averaged to estimate the general behavior of pH sensitivity as shown in Fig. 6. Error bars indicate the standard deviation from the average. The reason why the current at pH 7 was chosen is that the deprotonation of —SiOH takes place at pH 6.8. SiO_2 NP layer plays a role of charge collector, depending on pH of bulk solution as shown in Fig. 6(a), such that it may shift to positive or negative depending on the protonation/deprotonation of the surface hydroxyl groups. Decrease in pH induces protonation of —OH or $—O^-$, while increase in pH results in deprotonation of $—OH_2^+$ or —OH [17]. Hence, protonation/deprotonation are equivalent to positive/negative shift in pH gating voltage, thereby resulting in decreasing/increasing conductance of the underlying semiconducting SWCNTs. Furthermore, the surface functional groups of $—SiOH_2^+$ could be formed through the protonation of —SiOH below pH 2.3. In acidic environment, the conductance of SWCNT increases due to the hole doping of SWCNTs, but decreases due to the positive gate bias caused by SiO_2 NP layer. Generally, the effect of direct doping/undoping plays a dominant role in pH sensitivity [8,10] as shown in Fig. 6(b) and the SiO_2 NP layer may modulate the sensitivity particularly in acid region as well as linearize the response.

SWCNT multilayer devices were also characterized with ISFET scheme with the aid of external Ag/AgCl reference electrode as demonstrated in Fig. 2(a). A typical pH sensitivity of SWCNT ISFETs without and with SiO_2 NP layer is shown in Fig. 7. The explicit field-effects were observed regardless of the presence of SiO_2 NP as shown in Fig. 7(a) and (d), and I_D versus V_{DS} curves at the fixed

gate voltage of $V_G = -2.0$ V are shown in Fig. 7(b) and (e) in absence and presence of SiO_2 NPs, respectively. I_D was extracted at the fixed $V_{DS} = -1.0$ V and replotted as a function of pH as shown in Fig. 7(c) and (f). The pH sensitivity behavior is significantly different each other depending on the presence of SiO_2 NP layer. The SWCNT ISFET with SiO_2 NP showed a linear pH response, while the one without SiO_2 NP revealed an exponential relationship, which is the exactly same as SWCNT chemoresistors. This can be attributed to the adjusted sensitivity particularly in acidic region due to positive charge collector, thereby causing decrease in conductance.

Generally, SWCNT ISFET exhibited the same tendency as SWCNT chemoresistor as shown in Fig. 8: linear and exponential sensitivity in the presence and absence of SiO_2 NPs. Error bars denote the standard deviation. Indeed, SiO_2 NP layer linearizes the pH response in both SWCNT chemoresistor and ISFET. Furthermore, it is observed that the sensitivity in ISFETs increased compared to the chemoresistors in the presence of SiO_2 NP, whereas more sensitive response is shown only at acidic environment in ISFETs compared to the chemoresistors in the absence of SiO_2 NPs. With SiO_2 NPs, the p-channel formed by the use of external reference electrode diminishes due to positive charge of hydroxyl groups in

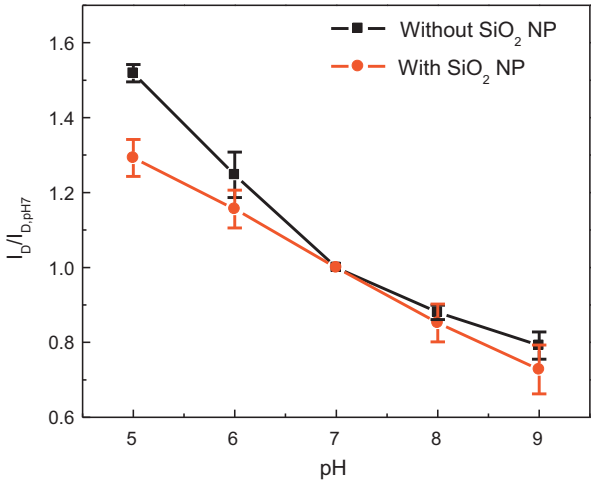

Fig. 8. pH sensitivity of SWCNT ISFETs normalized with the current at pH 7 at $V_G = -2.0$ V and $V_{DS} = -1.0$ V in the presence and absence of SiO_2 NP layers. Error bars indicate the standard deviation.

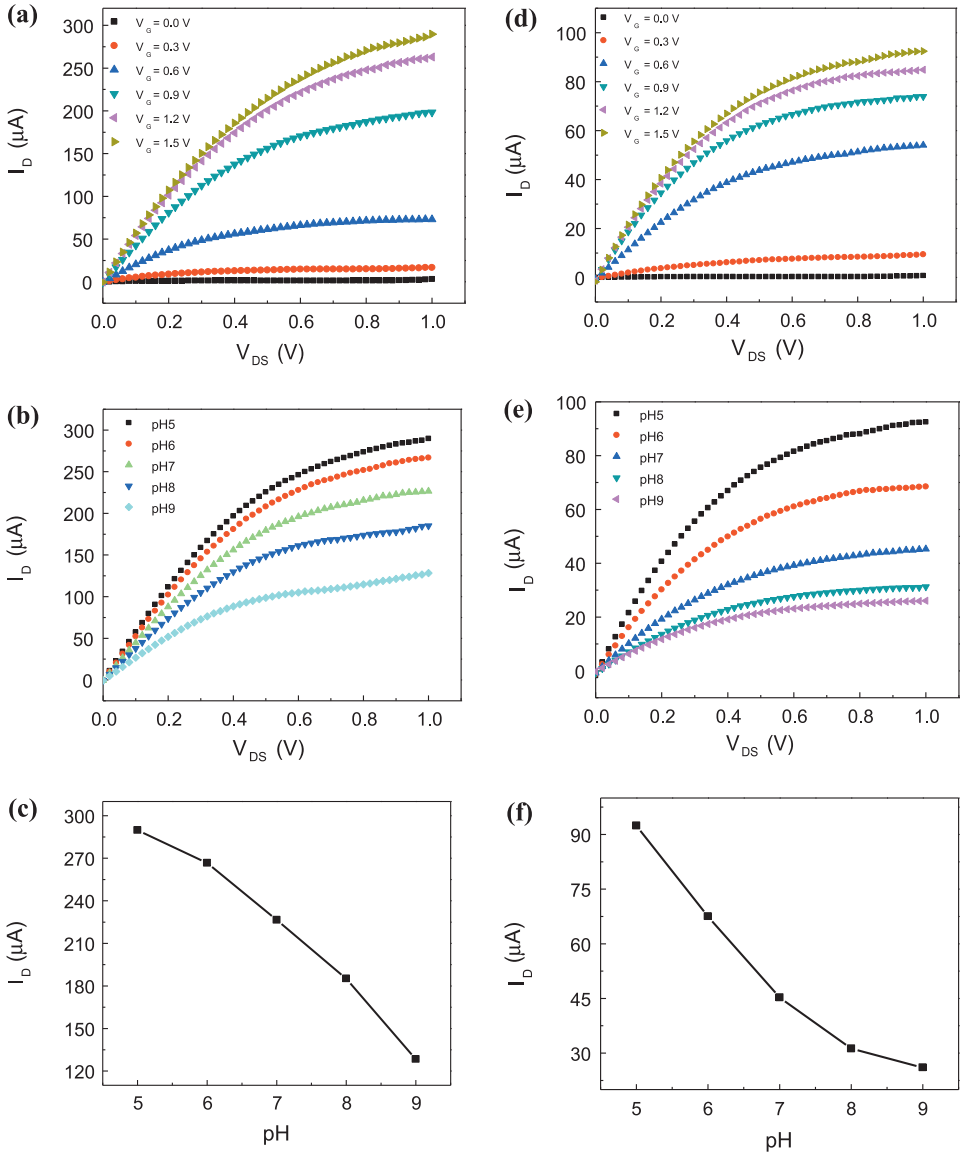

Fig. 9. A typical pH sensitivity of In_2O_3 NP ISFETs in the absence (a–c) and presence (d–f) of SiO_2 NP layer: (a and d) field-effect test at pH 5 buffer (b and e) drain currents at different pH buffers at the fixed $V_G = 1.5$ V, and (c and f) pH-responsive drain currents at the fixed $V_G = 1.5$ V and $V_{DS} = 1.0$ V.

SiO_2 NP, allowing less drain current in response to pH. Therefore, SiO_2 NP layer plays a role of forming conductive channel in SWCNT thin-film by collecting the charges in bulk solution. However, the other part of SWCNT can change their conductance by molecular doping/undoping. The use of external reference electrode enhances the conductive channel and reduces the effect of molecular doping/undoping. In addition, a higher sensitivity is observed at basic region in presence of SiO_2 NP layer than in absence of that. Deprotonation of carboxylic groups on SWCNTs becomes saturated at basic region without SiO_2 NP layer. On the other hand, deprotonation of hydroxyl groups on SiO_2 NPs takes place as illustrated in Fig. 6(a). Therefore, overall charge changes in SiO_2 NP layer leads to a higher sensitivity in the presence of SiO_2 NP layer.

Besides, In_2O_3NP ISFETs were constructed with and without SiO_2 NP layer and characterized only with ISFET characterization scheme. The different range of V_G was chosen to get reasonable field-effect at pH 5 buffer as shown in Fig. 9(a) and (d). I_D versus V_{DS} curve was extracted at the fixed $V_G = 1.5$ V in each pH buffer and replotted as shown in Fig. 9(b) and (e). I_D was extracted at the fixed $V_{DS} = 1.0$ V and replotted as a function of pH as shown in Fig. 9(c) and (f). It is clearly noticeable that the effect of SiO_2 NP layer is significantly different from the one observed in SWCNT ISFETs. Irrespective of the presence of SiO_2 NP, the overall behavior of decreasing conductance with increasing pH is observed. Without SiO_2 NP in Fig. 9(c), however, the ISFET is more sensitive to pH in basic region than acidic. On the other hand, the sensitivity is higher in acidic region than basic region in presence of SiO_2 NP layer as shown in Fig. 9(f).

The multiple In_2O_3NP ISFETs were tested, and I_D was normalized with the current at pH 5 as shown in Fig. 10. Error bars indicate the standard deviation from the average. The pH shift induces the change of protonation/deprotonation status in both In_2O_3NPs and SiO_2 NPs. Without SiO_2 NPs, the protonation status on In_2O_3NP surface determines the conductance of thin-film by space-charge model [9]. The pH decrease corresponds to less negative charges on the surface that makes space-charge layer thinner, leading to

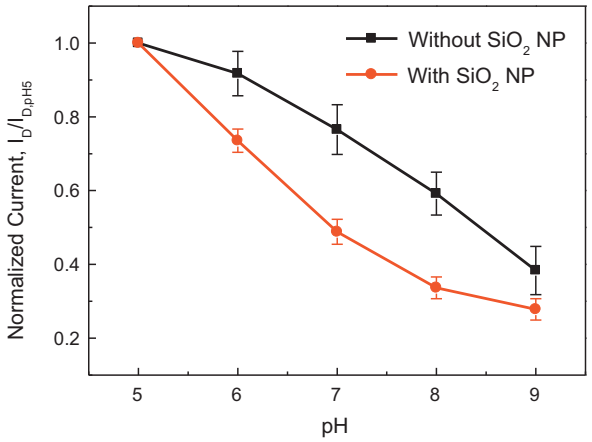

Fig. 10. pH sensitivity of In_2O_3 NP ISFETs normalized with the current at pH 5 at $V_G = 1.5$ V and $V_{DS} = 1.0$ V in the presence and absence of SiO_2 NP. Error bars indicate the standard deviation.

the reduced interparticle Schottky barrier. On the other hand, pH increase is equivalent to more negative charge on the surface, resulting in increased interparticle Schottky barrier. The reason why a higher sensitivity was found in basic region is that the isoelectric point of In_2O_3NP is 8.7 [18]. On the other hand, in the presence of SiO_2 NPs, the effect of SiO_2 NP comes into play applying gate voltage in a sense of FET. The pH decrease corresponds to the positive shift on SiO_2 NPs, which accumulates the conducting electrons, permitting more current. It is apparent that the sensitivity is higher in acidic region on the consideration that the silica surface keeps being protonated as mentioned earlier.

Nanomaterial thin-film pH sensors demonstrated in this study may show primarily either linear or exponential response due to the surface functional groups on the nanomaterials and electrochemical transducing thin-film structures. The nanomaterial thin-film devices that showed linear responses have potential

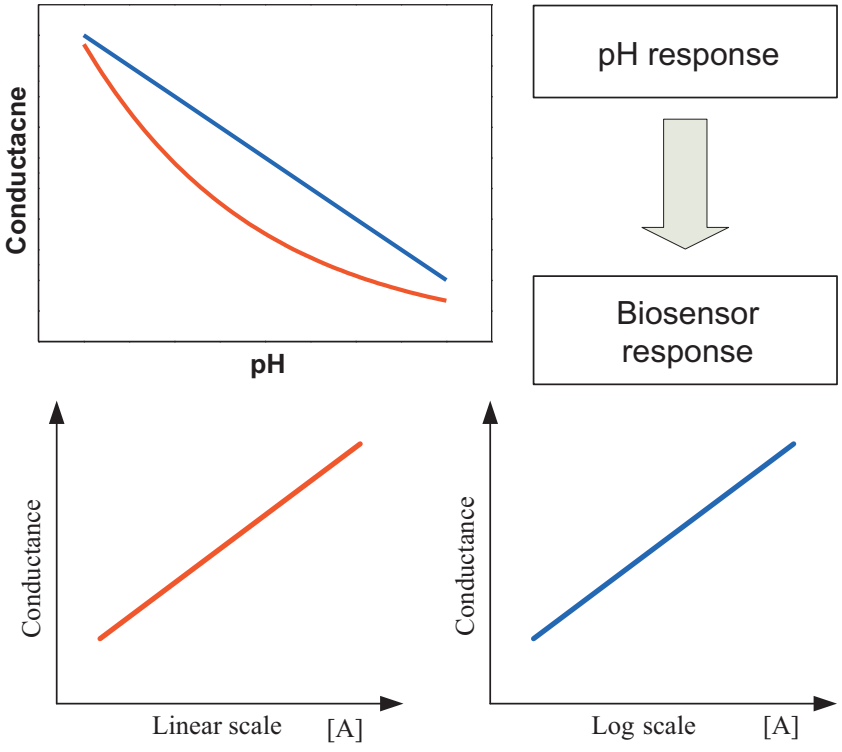

Fig. 11. The developmental scheme of electrochemical biosensors based on pH sensitivity behavior: different pH responses induce different type of response in biosensors.

applications to detect molecules that have a huge change during the biochemical reactions due to the log scale nature of pH. In addition, it can be applied for the detection of pathogens as a variety of bioassays. On the other hand, the nanomaterial thin-film devices exhibiting the exponential response to pH could be used to detect the biomolecules that have changes on the same order such as glucose. This development scheme of electrochemical biosensors based on pH sensing behavior is depicted in Fig. 11. Furthermore, there is more room to develop nanomaterial pH sensors either by functionalizing nanomaterials with various surface groups with more sensitive to chemical changes in sample solution or by exploiting elegant and novel nanostructured sensing elements. In the meantime, biosensors can be implemented in a variety of ways with which the sensing performance is maximized.

6. Conclusion

In conclusion, we have demonstrated tunable sensitivity and linearity of nanomaterial thin-film chemoresistors and ISFETs as pH sensors by employing SiO_2 NPs on top of function nanomaterial thin-film. In SWCNT resistors, SiO_2 NPs played the role of increasing resistivity, contact resistance, and sheet resistance by the surface adsorption. However, in SWCNT chemoresistors, it linearized pH sensitivity from exponential behavior in the device without SiO_2 NPs particularly in acidic region. This linearization is attributed to a positive shift in pH gating voltage in p-type SWCNTs. A similar effect was observed in SWCNT ISFETs, but it resulted in a higher sensitivity in presence of SiO_2 NPs. In the same way, SiO_2 NP played the role of changing surface charge, thereby gate voltage effect on the semiconducting In_2O_3NP layer. Without SiO_2 NP, In_2O_3NP ISFET is in the mode of space-charge. By adding SiO_2 NP layer, the pH gating voltage influences the conductivity of semiconducting nanomaterial thin-film layer and modulates the sensitivity which increases in acidic region. The different shape in sensitivity curves originates from the different isoelectric point of In_2O_3NP and SiO_2 NPs. pH sensitivity could be modulated further by employing different nanomaterials and nanostructures. Particularly, the ability of nanotechnology to tailor the size, structure, composition and surface chemistry may yield engineered nanomaterials or nanostructured sensing platform with a higher performance. The nanoengineered pH sensors could be a cornerstone in the future for developing biological sensors since many biochemical reactions accompany pH shift.

Acknowledgments

This work was supported in part by the Defense Advanced Research Projects Agency (DARPA) N/MEMS S&T Fundamentals program under grant no. HR001-06-1-0500 issued to the Micro/nano Fluidics Fundamentals Focus (MF3) Center. The authors would like to acknowledge the Nanofabrication Center and Characterization Facility at the University of Minnesota, which are supported by NSF through NNIN.

References

[1] Y. Liu, T. Cui, Ion-sensitive field-effect transistor based pH sensors using nano self-assembled polyelectrolyte/nanoparticle multilayer films, Sensors and Actuators B: Chemical 123 (2007) 148–152.
[2] W. Xue, T. Cui, Self-assembled carbon nanotube multilayer resistors and nanotube/nanoparticle thin-film transistors as pH sensors, Sensor Letters 6 (2008) 675–681.
[3] Y. Liu, A.G. Erdman, T. Cui, Acetylcholine biosensors based on layer-by-layer self-assembled polymer/nanoparticle ion-sensitive field-effect transistors, Sensors and Actuators A: Physical 136 (2007) 540–545.
[4] W. Xue, T. Cui, A thin-film transistor based acetylcholine sensor using self-assembled carbon nanotubes and SiO_2 nanoparticles, Sensors and Actuators B: Chemical 134 (2008) 981–987.
[5] D. Lee, T. Cui, Low-cost, transparent, and flexible single-walled carbon nanotube nanocomposite based ion-sensitive field-effect transistors for pH/glucose sensing, Biosensors and Bioelectronics 25 (2010) 2259–2264.
[6] J.H. Back, M. Shim, Ph-dependent electron-transport properties of carbon nanotubes, The Journal of Physical Chemistry B 110 (2006) 23736–23741.
[7] D. Lee, Y. Chander, S.M. Goyal, T. Cui, Carbon nanotube electric immunoassay for the detection of swine influenza virus H1N1, Biosensors and Bioelectronics 26 (2011) 3482–3487.
[8] D. Lee, T. Cui, pH-dependent conductance behaviors of layer-by-layer self-assembled carboxylated carbon nanotube multilayer thin-film sensors, Journal of Vacuum Science and Technology B 27 (2009) 842–848.
[9] M.E. Franke, T.J. Koplin, U. Simon, Metal and metal oxide nanoparticles in chemiresistors: does the nanoscale matter? Small 2 (2006) 301.
[10] D. Lee, T. Cui, Layer-by-layer self-assembled single-walled carbon nanotubes based ion-sensitive conductometric glucose biosensors, IEEE Sensors Journal 9 (2009) 449–456.
[11] W. Xue, Y. Liu, T. Cui, High-mobility transistors based on nanoassembled carbon nanotube semiconducting layer and SiO_2 nanoparticle dielectric layer, Applied Physics Letters 89 (2006) 163512.
[12] A. Walsh, J.L.F. Da Silva, S.-H. Wei, C. Korber, A. Klein, L.F.J. Piper, A. DeMasi, K.E. Smith, G. Panaccione, P. Torelli, D.J. Payne, A. Bourlange, R.G. Egdell, Nature of the band gap of In_2O_3 revealed by first-principles calculations and X-ray spectroscopy, Physical Review Letters 100 (2008) 167402.
[13] W. Xue, T. Cui, Characterization of layer-by-layer self-assembled carbon nanotube multilayer thin films, Nanotechnology 18 (2007) 145709.
[14] Y.H. Yoon, J.W. Song, D. Kim, J. Kim, J.K. Park, S.K. Oh, C.S. Han, Transparent film heater using single-walled carbon nanotubes, Advanced Materials 19 (2007) 4284–4287.
[15] R. Jackson, S. Graham, Specific contact resistance at metal/carbon nanotube interfaces, Applied Physics Letters 94 (2009) 012109.
[16] Y. Zhou, L. Hu, G. Grüner, A method of printing carbon nanotube thin films, Applied Physics Letters 88 (2006) 123109.
[17] J.P. Icenhower, P.M. Dove, Water behavior at silica surfaces, in: E. Papirer (Ed.), Adsorption on Silica Surfaces, CRC Press, 2000, pp. 277–295.
[18] M. Kosmulski, Pristine points of zero charge of gallium and indium oxides, Journal of Colloid and Interface Science 238 (2001) 225–227.

Biographies

Dongjin Lee received his B.S. and M.S. degrees from Korea University, Seoul, Korea in 2003 and 2005, respectively and his Ph.D. degree from the University of Minnesota in 2010. He is currently a Postdoctoral Research Associate at the Department of Mechanical Engineering, Korea Advanced Institute of Science and Technology (KAIST). From 2004 to 2005, he worked as a Guest Researcher at the Nanoscale Metrology Group, National Institute of Standards and Technology (NIST), MD, USA. His main research topics include micro- and nanoelectromechanical systems (M/NEMS), nanomaterials, flexible electronics, energy and bio application of nanostructures, and general nanotechnology.

Tianhong Cui received his B.S. degree from Nanjing University of Aeronautics and Astronautics in 1991, and Ph.D. degree from the Chinese Academy of Sciences in 1995. He is currently a Professor of Mechanical Engineering at the University of Minnesota. From 1999 to 2003, he was an assistant professor of electrical engineering at Louisiana Technical University. Prior to that, he was a STA fellow at the National Laboratory of Metrology, and served as a postdoctoral research associate at the University of Minnesota and Tsinghua University. He received research awards including the Nelson Endowed Chair Professorship from the University of Minnesota, the Research Foundation Award from Louisiana Tech University, the Alexander von Humboldt Award in Germany, and the STA & NEDO fellowships in Japan. His current research interests include MEMS/NEMS, nanotechnology, and polymer electronics.